OPEN

Effects of Rivastigmine on Brain Functional Networks in Patients With Alzheimer Disease Based on the Graph Theory

Jiangtao Zhang, MS, Jianan Cheng, MS,† and Hua Yang, MS**

Objective: The aim of this study was to explore the effect of rivastigmine on brain function in Alzheimer disease (AD) by analyzing brain functional network based on the graph theory.

Methods: We enrolled 9 patients with mild to moderate AD who received rivastigmine treatment and 9 healthy controls (HC). Subsequently, we used resting-state functional magnetic resonance imaging data to establish the whole-brain functional network using a graph theory–based analysis. Furthermore, we compared systemic and local network indicators between pre- and posttreatment.

Results: Patients with AD exhibited a posttreatment increase in the Mini-Mental State Examination scores and a decrease in the Alzheimer's Disease Assessment Scale cognitive subscale scores and activities of daily living. The systemic network for HC and patients with AD had good pre- and posttreatment clustering coefficients. There was no change in the C_p, L_p, Gamma, Lambda, and Sigma in patients with AD. There were no significant between-group differences in the pre- and posttreatment systemic network measures. Regarding the regional network, patients with AD showed increased betweenness centrality in the bilateral caudate nucleus and right superior temporal pole after treatment with rivastigmine. However, there was no between-group difference in the pre- and posttreatment betweenness centrality of these regions. There were no significant correlations between regional network measure changes and clinical score alterations in patients with AD.

Conclusions: There are similar systemic network properties between patients with AD and HC. Rivastigmine cannot alter systemic network attributes in patients with AD. However, it improves the topological properties of regional networks and between-node information transmission in patients with AD.

Key Words: Alzheimer disease, rivastigmine, rs-fMRI, brain network, graph theory

(*Clin Neuropharm* 2021;44: 9–16)

Alzheimer disease (AD), which is a primary degenerative brain disease, is characterized by unknown etiology, hidden onset, and gradual disease progression.[1] Clinically, there is a progressive decline in various cognitive functions in patients with AD, including episodic memory, orientation, and executive function. Alzheimer disease remains incurable; however, some drugs can improve its clinical symptoms or postpone disease progression. Common drugs used for treating mild to moderate AD include cholinesterase inhibitors such as donepezil, rivastigmine, and galantamine. Among them, rivastigmine has superior clinical efficacy because it simultaneously inhibits acetylcholinesterase and butyrylcholinesterase activities.[2,3] However, the mechanism underlying its clinical efficacy regarding brain function remains unclear, with only few related studies available.

A study that used positron emission tomography using (18) F-fluorodeoxyglucose reported that rivastigmine could improve the hippocampal metabolic rate.[4] Specifically, during episode memory tasks, rivastigmine can enhance and inhibit neural activity in the right fusiform gyrus and posterior cingulate cortex, respectively.[5] Moreover, magnetic resonance spectroscopy studies reported that rivastigmine can accelerate the frontal cortical metabolic rate.[6] These previous studies focused on the role of rivastigmine in functional metabolism in the local brain area. With the development of neuroimaging, resting-state functional magnetic resonance imaging (rs-fMRI) demonstrated connection losses between brain systems in patients with AD,[7] which is mainly characterized by abnormal structures and functions in different brain areas.[8] The brain is a complex organ, and tasks are synergic consequences of the corresponding brain functional areas; therefore, there is a need to examine overall brain function. Recent graph theory–based brain network studies have reported brain network topological alterations in patients with AD,[9] specifically imbalanced functional differentiation and integration. The graph theory can reflect the brain's ability to integrate and process information,[8] with the brain being regarded as a complicated network comprising largely interconnected areas.[10] The brain can be described using a group of well-defined nodes structured for perfect interactions between segregation and integration of functionally specialized areas.[11] Specifically, betweenness centrality is a factor that represents node importance, which is indicated by the shortest path number through the node. Moreover, a brain node with a high centrality degree could serve as the center of information transmission. Typically, the clustering degree and local information transmission capability of the network are measured using the clustering coefficient (C_p).[12] The mean length of the shortest internode path in the network is described as the characteristic path length (L_p), which also determines the systemic network transmission ability. Notably, a small-world network is characterized by highly clustered vertex assemblies and a small number of intercluster systemic shortcuts, which facilitate functional synchronization.[13]

Resting-state fMRI is used to identify changes in brain regions based on MRI signal alterations induced by different resting-state blood oxygen levels. It is a nonradioactive and noninvasive method with high temporal and spatial resolution.[14] Previous studies using rs-fMRI and graph theory–based analyses have reported abnormal brain and topological structures, with regard to functional network topology, in patients with AD. Furthermore, these patients present with remarkable alterations in the small-world,

*Department of Geriatrics, and †Department of Pharmacy, Tongde Hospital of Zhejiang Province, Hangzhou, Zhejiang, China.

Address correspondence and reprint requests to Jianan Cheng, MS, Departments of Pharmacy, Tongde Hospital of Zhejiang Province, 234 Gucui Road XihuDist, Hangzhou 310012, China;
E-mail: chw1233210@163.com; Hua Yang, MS, Department of Geriatrics, Tongde Hospital of Zhejiang Province, Hangzhou, Zhejiang, China;
E-mail: 843329268@qq.com

Conflicts of Interest and Source of Funding: This work was funded by grants from the Medical Health Science and Technology Project of Zhejiang Provincial Health Commission (2015KYB073), the Traditional Chinese Medicine Technology Project of Zhejiang Province (2015ZA018) to Jiangtao Zhang, and the Project of Basic Public Welfare Research of Zhejiang (LGF18H090021) to Jianan Cheng. The authors have no conflicts of interest to declare.

DOI: 10.1097/WNF.0000000000000427

network efficiency, node degree, and betweenness centrality.[9] Moreover, brain network topological indices are associated with favorable sensitivity and specificity, which can distinguish patients with AD from cognitively normal elderly individuals.[9,14,15] In addition, the graph theory has been adopted to identify biomarkers of depression,[16] schizophrenia,[17] obsessive-compulsive disorder,[18] and epilepsy.[19] However, the effect of acetylcholinesterase inhibitors in the brain network of patients with AD has not been investigated using rs-fMRI and the graph theory.

Therefore, this longitudinal study aimed to use rs-fMRI to determine functional network topological alterations in patients with AD before and after treatment with rivastigmine at both systemic and local levels. Specifically, we aimed to determine the rivastigmine effect on the system and local functional networks in the brain of patients with AD.

MATERIALS AND METHODS

Participants

In this study, patients with AD were diagnosed according to the AD Diagnostic Criteria for "Possible or Probable AD" established by the National Institute of Neurological and Communicative Disorders and Stroke, as well as the Alzheimer's Disease and Related Disorders Association. We included eligible patients with AD, regardless of sex, based on the following inclusion criteria: (1) age 65 to 85 years without any potential for pregnancy; (2) having a Mini-Mental State Examination (MMSE) score of 10 to 24 points and a Clinical Dementia Rating (CDR) score greater than 1; (3) having elementary and higher education, ability to read and write in simplified Chinese, and sufficient vision and hearing abilities for reliable completion of research evaluation; and (4) having reliable caregivers who could provide information and supervise accurate medicine intake.

The exclusion criteria were as follows: (1) patients with AD showing neuropsychiatric or secondary dementia, (2) patients currently or planning to participate in an AD drug trial, (3) patients who previously received AD antibody therapy, and (4) patients with anticholinergic or anticonvulsive medication dose changes within 4 weeks before the baseline assessment. In addition, the craniocerebral MRI exclusion criteria were as follows: (1) presenting clinically significant cortical or subcortical infarctions on MRI, (2) having clinically significant infarcts in critical sections of the subcortical gray matter [including the hippocampal region, lateral hypothalamic area, and left caudate nucleus (CAU)], (3) having clinically significant multiple lacunar infarcts in the white matter (≥2 infarcts), and (4) having extensive white matter damage indicative of Binswanger disease or other severe white matter abnormalities. We did not exclude patients showing mild to moderate white matter damage that was consistent with the patients' age and was not associated with other radiological findings or clinically relevant conditions.

Drug Treatment and Efficacy Evaluation

The patients received oral rivastigmine (1.5 mg per capsule, 28 capsules per package, Novartis Farmaceutica SA, Spain) for 24 weeks at a starting dose of 1.5 mg twice a day (BID) at breakfast and dinner for the first 2 weeks, 3 mg BID from the third week, and 4.5 mg BID from the fifth week, with the maximum rivastigmine dose being 12 mg/d. Typically, patients who did not achieve the minimum target daily dose of 6 mg rivastigmine were withdrawn from the study.

Assessment Tools for Clinical Curative Effect

We used MMSE[20] and the Alzheimer's Disease Assessment Scale cognitive subscale (ADAS-cog)[21] to assess cognitive function, CDR[22] to assess dementia severity, Activity of Daily Living Scale (ADL)[23] to assess daily functioning, and Neuropsychiatric Inventory (NPI)[24] to assess psycho-behavioral symptoms in patients with AD.

Healthy Controls

We enrolled healthy individuals aged 65 to 85 years with normal overall cognitive function, no significant memory or other cognitive dysfunction, MMSE score greater than 24, and CDR score of 0. Moreover, the exclusion criteria for healthy controls (HC) were similar to those for patients with AD.

Between January 2016 and June 2018, we enrolled 13 right-handed patients with AD from Tongde Hospital, Zhejiang Province, China. These patients were treated with rivastigmine for 24 weeks; moreover, they underwent clinical assessments (including the CDR, MMSE, ADAS-cog, NPI, and ADL) and MRI scans at baseline and week 24. Two patients dropped out of the study due to intolerable nausea, which is a treatment adverse effect. Two patients showed excessive head movement during MRI scans, which rendered the data unusable. Finally, 9 patients completed the study. Consequently, we selected 9 normal elderly people matched according to age, sex, and education level as normal controls (HC), and they underwent clinical assessments and MRI scans upon enrollment. This study was approved by the ethics committee; moreover, all participants provided written informed consent for study participation.

Magnetic Resonance Imaging Data Acquisition

Magnetic resonance imaging data were obtained using a 3.0-Tesla scanner (Magnetom Verio, Siemens, Erlangen, Germany). The head was padded with dense and easeful foam padding to extensively reduce head motion; further, earplugs were worn to decrease the scanning noise. Subsequently, we applied the 3-dimensional T1-weighted magnetization-prepared rapid gradient-echo sequence using the following parameters (repetition time of 1900 milliseconds, echo time of 2.48 milliseconds, inversion time of 900 milliseconds, flip angle of 9°, field of view of 250 mm × 250 mm, matrix of 512 × 512, slice thickness of 1 mm, no gap, and a slice number of 176) to yield high-resolution sagittal structural images. Furthermore, we used the gradient-echo echo planar imaging sequence to obtain resting-state axial functional blood-oxygen-level-dependent (BOLD) images using the following parameters (repetition time/echo time of 2000/30 milliseconds, flip angle of 90°, field of view of 220 mm × 220 mm, matrix of 64 × 64, slice thickness of 4 mm, gap of 0.8 mm, slice number of 30, and 160 volumes). During the scan, the participants were asked to close their eyes, relax, minimize their motion, keep their mind relaxed, and remain awake. Subsequently, all the obtained MRI images were visually examined to ensure only artifact-free images were included for analyses.

Preprocessing of fMRI Data

Resting-state BOLD data were preprocessed using Statistical Parametric Mapping 12 (http://www.fil.ion.ucl.ac.uk/spm) and Data Processing Assistant for Resting-State fMRI (http://rfmri.org/DPARSF).[25] Typically, for each participant, the first 10 volumes were eliminated to ensure that the signals reach equilibrium, with all participants being able to adjust the noise during scanning. The remaining volumes were adjusted according to the between-slice acquisition time delay. Subsequently, the motion between different time points was corrected through realignment.

For each volume, we calculated the head motion parameters by determining the translation in each direction and the angular rotation on each axis. Typically, the BOLD data of all the participants lay within the defined motion thresholds (ie, translational or rotational motion parameters <3 mm or <3°). Moreover, we calculated the framewise displacement, which indicated volume-to-volume changes in head position. In addition, we excluded several unexpected covariates (including the Friston 24 model–based estimated motion parameters, linear drift, white matter signal, and cerebrospinal fluid signal) from the data. Recent studies have indicated that the head motion–induced signal spike could significantly affect the eventual rs-fMRI results, even after regressing out linear motion parameters.[26] Therefore, we further regressed out the spike volumes in the presence of a specific volume framewise displacement greater than 0.5. Subsequently, the datasets were band-pass filtered, with the frequencies ranging from 0.01 to 0.1 Hz. During normalization, each individual's structural images were coregistered with the mean functional image, followed by segmenting and normalizing the transformed structural images using a high-level nonlinear warping algorithm to the Montreal Neurological Institute space based on the diffeomorphic anatomical registration through the exponentiated Lie algebra technique.[27] Finally, all the filtered functional volumes were normalized to Montreal Neurological Institute space using the previously mentioned deformation parameters and resampled into a 3-mm cubic voxel.

Network Construction

The whole-brain functional network, which comprised nodes (brain regions) and internode edges (functional connectivity), was constructed using GRETNA software (http://www.nitrc.org/projects/gretna). Subsequently, the brain was segmented into 90 cortical and subcortical regions of interest (ROIs) (considered as a group of nodes in this network analysis) using the automated anatomical labeling template to define the network nodes.[28] Each hemisphere contained 45 ROIs. For each participant, the BOLD time series of all voxels in each ROI was averaged to obtain the representative value. Moreover, we computed the Pearson correlation coefficients among the average time series of all potential node pairs to define the network edges, with a 90 × 90 correlation matrix being generated for each participant. Finally, the correlation matrix thresholds were determined (refer to the threshold selection below for more details) and converted into binary matrices (ie, adjacency matrices). If the absolute Pearson correlation coefficient of region i with region j was more than the threshold, then entry $a_{ij} = 1$; otherwise, $a_{ij} = 0$.

Network Analysis

For network analysis, we applied a series of sparsity thresholds, which were considered as the ratios of the division result of the existing edge number by the maximum potential edge number in the network to all correlation matrices. This method ensures that all the constructed networks had equal edge numbers, which allows assessment of between-group differences in the relative network organization.[29,30] This study used sparsity thresholds ranging from 0.10 to 0.34 at intervals of 0.01, as previously described.[31–34] Typically, this thresholding method was considered depending on the possible estimation of the constructed networks with regard to small-worldness and possession of sparse properties involving the potential minimum spurious edge number.

Systemic and regional network measures were computed for each brain network at every sparsity threshold.

On the one hand, systemic measures included 5 small-world property metrics[35]: C_p (measured degree of local density or network cliquishness), L_p (measured degree of average whole-network connectivity or routing efficiency), normalized clustering coefficient (Gamma; the real: random network clustering coefficient ratio), normalized characteristic path length (Lambda; the real: random network characteristic path length ratio), and small-worldness [Sigma = Gamma/Lambda](a scalar quantized small-worldness network measure).

On the other hand, regional measures were presented as betweenness centrality [refer to the reviews[36] for uses and interpretations]. Typically, betweenness was considered as the fraction of each characteristic path passing the given network node, which could capture the node effect on the information flow among the other network nodes. Therefore, brain areas with large betweenness centrality were regarded as bridging hubs crucially involved in connecting the disparate network parts. Moreover, the area under the curve was calculated for all network metrics, which provided a summarized scalar for characterizing brain network topology. The integrated area under the curve metric was not dependent on single threshold selection. Therefore, it was sensitive to topological changes associated with brain disorders; moreover, it has been widely applied to investigate brain networks.[31–34]

Statistical Analysis

All statistical analyses were performed using SPSS 19.0. (SPSS, Chicago, Illinois). Two-sample t tests were used for between-group comparisons of age, education, baseline CDR scores, and MMSE scores. Between-group sex differences were determined using the Pearson χ^2 test. For patients with AD, pre- and posttreatment changes in the CDR, MMSE, ADAS-cog, NPI, and ADL scores were evaluated using paired t tests.

Moreover, 2-sample t tests were used to explore between-group differences in the systemic and regional network measures. Furthermore, paired t tests were used to examine pre- and posttreatment changes in the 5 small-world property metrics and betweenness centrality. Finally, the associations between significant posttreatment changes in network measures and clinical scores of patients with AD were assessed using Pearson correlation analyses.

TABLE 1. Demographic and Clinical Characteristics of the Sample

Characteristics	Patients With AD (n = 9)	HC (n = 9)	Statistics	*P*
Age, y	72.7 ± 12.6	73.0 ± 12.2	$t = -0.057$	0.955*
Sex (female/male)	7/2	7/2	$\chi^2 = 0$	1†
Education, y	9.9 ± 4.2	10.3 ± 3.4	$t = -0.246$	0.809*
CDR (baseline)	1.4 ± 0.5	0 ± 0	$t = 8.222$	<0.001*
CDR (24 wk)	1.4 ± 0.5	—		
MMSE (baseline)	14.6 ± 6.0	29.6 ± 0.9	$t = -7.468$	<0.001*
MMSE (24 wk)	16.6 ± 6.2	—		
ADAS-cog (baseline)	28.6 ± 10.1	—		
ADAS-cog (24 wk)	24.1 ± 10.7	—		
NPI (baseline)	0 ± 0	—		
NPI (24 wk)	0 ± 0	—		
ADL (baseline)	35.1 ± 15.3	—		
ADL (24 wk)	29.6 ± 13.0	—		

The data are shown as mean ± SD.

*The *P* values were obtained by 2-sample *t* tests.

†The *P* value was obtained by Pearson χ^2 test.

RESULTS

Characteristics of the Samples

Table 1 presents the demographic and clinical characteristics of each participant. There were no significant between-group differences in age (2-sample t test, $t = -0.057$, $P = 0.955$), sex (χ^2 test, $\chi^2 = 0$, $P = 1$), and education (2-sample t test, $t = -0.246$, $P = 0.809$). However, patients with AD showed significantly higher baseline CDR scores (2-sample t test, $t = 8.222$, $P < 0.001$) and lower baseline MMSE scores (2-sample t test, $t = -7.468$, $P < 0.001$) compared with those of HC. After treatment, patients with AD showed increased MMSE scores (paired t test, $t = 2.502$, $P = 0.037$), as well as decreased ADAS-cog (paired t test, $t = -3.412$, $P = 0.009$) and ADL scores (paired t test, $t = -3.454$, $P = 0.009$) (Fig. 1). However, there was no significant posttreatment change in the CDR and NPI scores.

Changes in the Systemic Network Measures

Within the defined threshold range, functional brain networks in HC and patients with AD had good pre- and posttreatment clustering coefficients (ie, Gamma > 1). However, there were almost similar characteristic path lengths (ie, Lambda ≈ 1) with those of the corresponding random networks, which is indicative of the characteristic small-world topology (ie, Sigma > 1) (Fig. 2). Moreover, there was no posttreatment change in the C_p, L_p, Gamma, Lambda, and Sigma ($P > 0.06$) (Fig. 3) of patients with AD. Furthermore, there were no significant between-group differences in the pre- and posttreatment systemic network measures($P > 0.13$) (Fig. 3).

Alterations in Regional Network Measures

Patients with AD showed a posttreatment increase in betweenness centrality in the bilateral CAU and right superior temporal pole (TPOsup) (Fig. 4). However, there were no significant between-group differences in the pre- and posttreatment betweenness of these regions ($P > 0.11$) (Fig. 4). In addition, there were no significant correlations between posttreatment regional network measure changes and clinical score alterations in patients with AD ($P > 0.07$).

DISCUSSION

Our findings indicated that rivastigmine treatment for patients with AD increased their MMSE scores and decreased the ADAS-cog and ADL scores. There were no marked posttreatment changes in the systemic network measures of patients with AD, which is suggestive of the characteristic small-world topology. Regarding regional networks, there were evident changes in the betweenness centrality of multiple nodes. Specifically, there was posttreatment enhancement in betweenness centrality in the bilateral CAU and TPOsup in patients with AD; however, it did not show a significant between-group difference. These findings could facilitate the understanding of the neural mechanisms underlying AD treatment using rivastigmine based on brain functional networks.

We observed a posttreatment improvement in the MMSE, ADAS-cog, and ADL scores, which was consistent with previous findings[37–39] on the effects of rivastigmine on AD.

In this study, the whole-brain network of patients with AD was analyzed using the C_p, L_p, Gamma, Lambda, and Sigma, which showed no significant between-group differences or posttreatment changes. They all had small-world properties, which could be attributed to the system network in patients with mild to moderate AD not being disrupted and being capable of information processing, as reported in previous studies.[40] However, there was no significant posttreatment change in the systemic network, which indicated that rivastigmine lacked an obvious effect on the systemic network. These findings could be attributed to our very small sample not allowing for sufficient power to reveal significant changes in the whole-brain network measures in patients with AD after rivastigmine treatment. Alternatively, rivastigmine treatment for dementia may not affect the underlying disease progression in AD.[41] In addition, compensation from other brain regions or loops could lead to the seemingly "normal" systemic network given that the brain was highly conserved and robust.[11]

Nonetheless, regarding the regional network measures, there was a posttreatment increase in the betweenness centrality in the bilateral CAU and right TPOsup of patients with AD. Typically, the CAU, which comprises bilateral subcortical gray matter structures, is a part of the basal ganglia and frontal striatum network; moreover, it is involved in motor, emotional, and cognitive functions.[42] Moreover, the CAU is substantially involved in high-level human cognition.[43] Specifically, as described by Alexander et al[44] in 1986, it plays a role in advanced cognitive processes through the dorsolateral prefrontal circuit. Furthermore, the CAU is involved in an active feedback loop[45] for guiding attention. In addition, it is related to both motor and nonmotor functions, including set shifting, spontaneous responses, rule learning, contingency action, planning, language, speech processing, and other cognitive processes.[46–48] Previous studies have reported a marked reduction in the CAU volume in patients with AD compared with that in HC.[49,50] Patients with AD have also presented a marked decrease in the galanin binding site number in the CAU.[51] Furthermore, this study suggested that the pretreatment betweenness centrality in the CAU of patients with AD was lower than that of HC. There are numerous cholinergic neurons distributed in the CAU[52–55]; moreover, acetylcholine is an important neurotransmitter in the central cholinergic nervous system. In addition, changes in acetylcholine may directly affect learning, memory, and cognition functions.[56,57] Previous studies have reported cholinergic neurotransmitter dysfunction in the CAU of patients with AD.[58] In addition, this study showed that rivastigmine could enhance the betweenness centrality

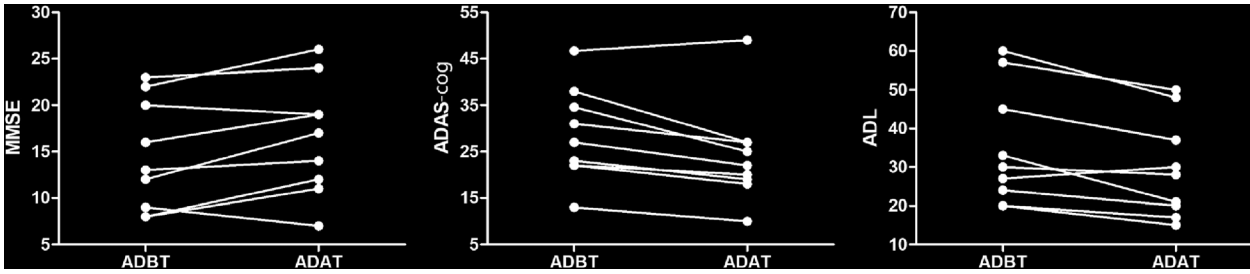

FIGURE 1. Posttreatment changes in the clinical assessments. ADAT, patients with AD after treatment; ADBT, patients with AD before treatment.

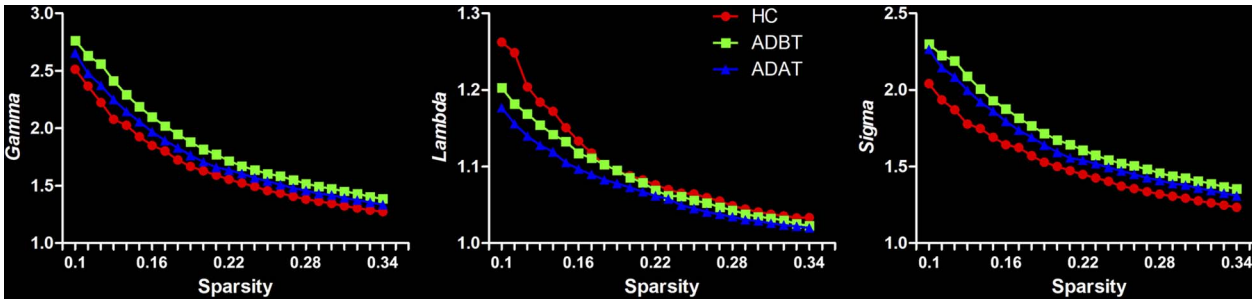

FIGURE 2. Small-world property metrics as a function of sparsity thresholds. Regarding the defined threshold range, HC and patients with AD before and after treatment showed normalized clustering coefficients (Gamma) and small-worldness (Sigma) substantially greater than 1, and normalized characteristic path lengths (*Lambda*) approximately equal to 1. This was indicative of a typical small-world topology. ADAT, patients with AD after treatment; ADBT, patients with AD before treatment.

of the CAU, which suggests that it might improve AD symptoms by promoting the information transmission center function of the CAU and that it exerts beneficial effects on bilateral CAU. Therefore, rivastigmine could show specific selectivity for the CAU.

The temporal pole, which is a part of the cerebral cortex, is involved in multimodal sensory integration[59,60] and is associated with various advanced social-emotional cognition function including language processing,[61,62] face processing,[63] emotions,[64–66] subjective assessment,[67] and semantic integration.[68,69] Moreover, the temporal pole is a major component of the temporal sensory system, which includes the visual, auditory, olfactory, and gustatory systems.[70,71] Different functional roles of the left and right temporal poles have been described. Specifically, the left temporal pole is mainly involved in perceptual decoding, semantic processing, and conceptualization.[71] However, the right temporal pole is mostly associated with social-emotional cues of multisensory perceptual stimulations.[72] Typically, the right temporal pole is involved in individual and episodic memories, which are closely associated with social-emotional memories.[73] Therefore, nonverbal semantic processing is more susceptible after right temporal pole damage.[74] Notably, rivastigmine treatment for patients with AD could improve regional cerebral perfusion in the temporal areas.[75,76] Moreover, this study found that rivastigmine improved the betweenness centrality in the right TPOsup. Therefore, rivastigmine might improve episodic memories of patients with AD by enhancing the information transmission center in the right TPOsup. Moreover, the temporal pole could receive highly processed visual signals from the perirhinal cortex and communicate with the amygdala and thus participate in the ventral visual stream during visual information processing.[69,77,78] In addition, Wezenberg et al[79] reported that rivastigmine could improve cognitive and visuospatial functions in healthy elderly individuals, which suggests that the posttreatment betweenness centrality improvement in the right TPOsup might promote cognitive and visuospatial functions in patients with AD.

This study showed no between-group difference in the pre- and posttreatment betweenness centrality between the CAU and TPOsup. However, there was a significant posttreatment increase in the betweenness centrality of both brain regions, which suggests that rivastigmine can improve information processing efficiency in the local brain regions of patients with AD. Therefore, we assume that rivastigmine exerts a therapeutic effect on AD

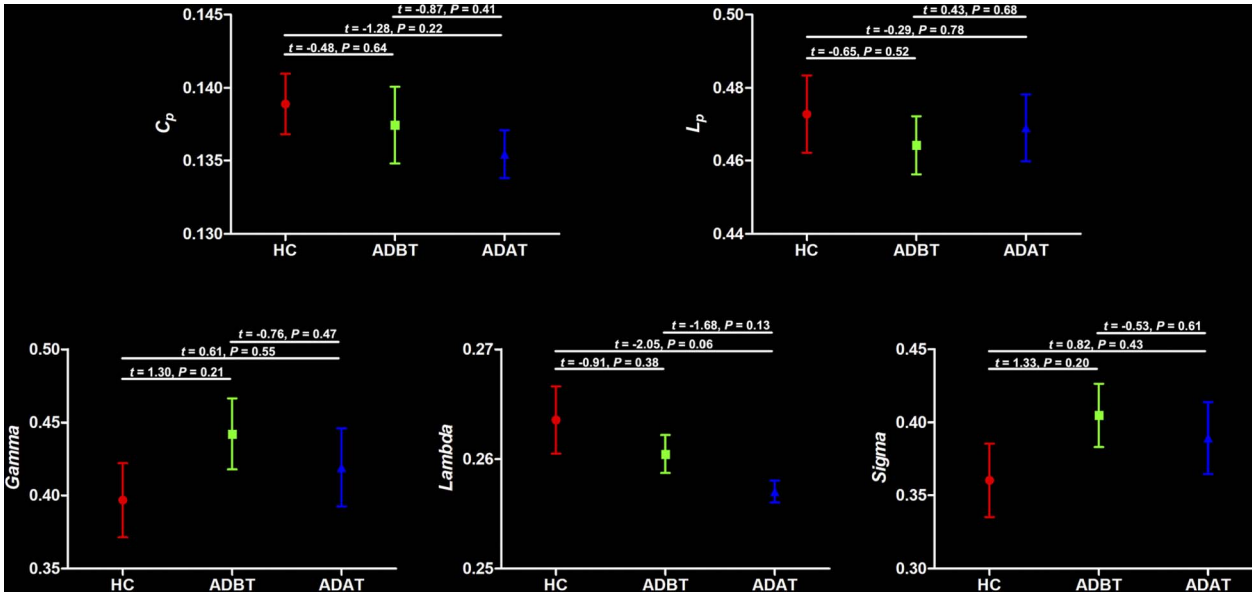

FIGURE 3. Changes in systemic network measures between the pre- and posttreatment measurements and between patients and controls. Error bars represent standard errors. ADAT, patients with AD after treatment; ADBT, patients with AD before treatment.

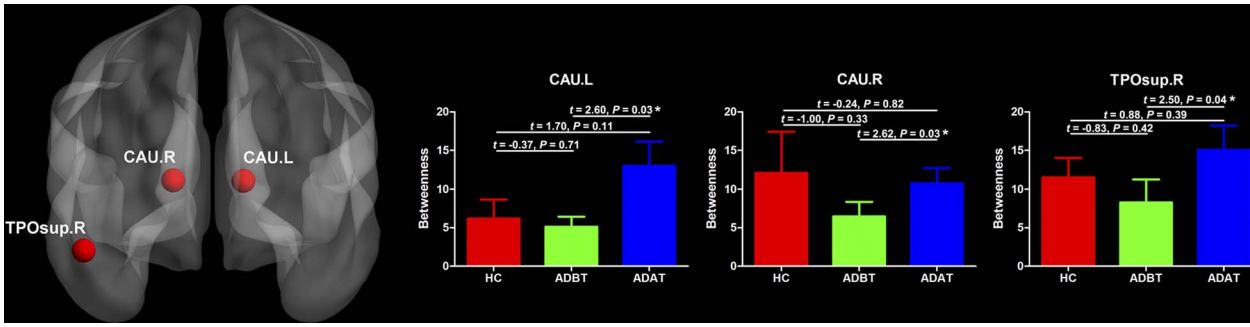

FIGURE 4. Changes in regional network measure between pre- and posttreatment measurements and between patients and controls. Error bars represent standard errors. ADAT, patients with AD after treatment; ADBT, patients with AD before treatment; L, left; R, right; TPOsup, superior temporal pole.

through compensation of normal encephalic regions; however, such compensation is limited and would present as decompensation once the compensation declines at a rate slower than the functional decline of AD-affected encephalic regions. As suggested in some studies, although rivastigmine can significantly improve the MMSE score in the first few months of AD treatment, the MMSE score would continue to decrease thereafter.[41,80] Based on the above, rivastigmine can only delay rather than reverse the course of AD.

This study has several limitations. First, this study had a small sample size, with some of the enrolled patients withdrawing from the study. This was attributed to the difficulty in following up the drug therapy for patients with AD and their inability to cooperate during MRI scans. Second, the data were not normally distributed, which was largely caused by data skewness resulting from the small sample size. Nonetheless, this exploratory longitudinal study still provides useful clinical suggestions for reference. Third, the elderly often develop underlying diseases requiring multiple drugs, which might have affected our results. Therefore, future studies should apply more effort to enroll only patients with AD. Fourth, the sample size for regional network analysis was small; moreover, as previously suggested, differences in the parcellation strategy might result in changes in the graph-theoretical metrics.[81,82] This could lead to false-positive results; however, the automated anatomical labeling template (90 brain regions) currently remains the classic method.[28,83] Nonetheless, the results of this study have several implications. In our next study, we will use a larger sample size.

Taken together, this study, which was based on the rs-fMRI technique and graph theory–based analysis, found that rivastigmine did not alter systemic brain network properties of the brain network in patients with AD. However, rivastigmine could increase the betweenness centrality in the CAU and right TPOsup, which suggests that it could be used as a potential biomarker for monitoring the efficacy of AD drugs. This could also contribute to guiding individualized treatments. However, these findings should be further verified given the small sample size of this study.

ACKNOWLEDGMENT

We would like to thank all the radiologists in Tongde Hospital of Zhejiang Province for providing assistance in scanning.

REFERENCES

1. Hojjati SH, Ebrahimzadeh A, Khazaee A, et al. Predicting conversion from MCI to AD using resting-state fMRI, graph theoretical approach and SVM. *J Neurosci Methods* 2017;282:69–80.
2. Bullock R, Touchon J, Bergman H, et al. Rivastigmine and donepezil treatment in moderate to moderately-severe Alzheimer disease over a 2-year period. *Curr Med Res Opin* 2005;21(8):1317–1327.
3. Inglis F. The tolerability and safety of cholinesterase inhibitors in the treatment of dementia. *Int J Clin Pract Suppl* 2002;(127):45–63.
4. Potkin SG, Anand R, Fleming K, et al. Brain metabolic and clinical effects of rivastigmine in Alzheimer disease. *Int J Neuropsychopharmacol* 2001; 4(3):223–230.
5. Richter N, Beckers N, Onur OA, et al. Effect of cholinergic treatment depends on cholinergic integrity in early Alzheimer disease. *Brain* 2018; 141(3):903–915.
6. Modrego PJ, Pina MA, Fayed N, et al. Changes in metabolite ratios after treatment with rivastigmine in Alzheimer's disease: a nonrandomised controlled trial with magnetic resonance spectroscopy. *CNS Drugs* 2006; 20(10):867–877.
7. Dennis EL, Thompson PM. Functional brain connectivity using fMRI in aging and Alzheimer's disease. *Neuropsychol Rev* 2014;24(1):49–62.
8. Reid AT, Evans AC. Structural networks in Alzheimer's disease. *Eur Neuropsychopharmacol* 2013;23(1):63–77.
9. delEtoile J, Adeli H. Graph theory and brain connectivity in Alzheimer's disease. *Neuroscientist* 2017;23(6):616–626.
10. Sporns O, Chialvo DR, Kaiser M, et al. Organization, development and function of complex brain networks. *Trends Cogn Sci* 2004;8(9):418–425.
11. Tononi G, Sporns O, Edelman GM. A measure for brain complexity: relating functional segregation and integration in the nervous system. *Proc Natl Acad Sci U S A* 1994;91(11):5033–5037.
12. Khazaee A, Ebrahimzadeh A, Babajani-Feremi A. Application of advanced machine learning methods on resting-state fMRI network for identification of mild cognitive impairment and Alzheimer's disease. *Brain Imaging Behav* 2016;10(3):799–817.
13. Wang J, Wang L, Zang Y, et al. Parcellation-dependent small-world brain functional networks: a resting-state fMRI study. *Hum Brain Mapp* 2009; 30(5):1511–1523.
14. Khazaee A, Ebrahimzadeh A, Babajani-Feremi A. Identifying patients with Alzheimer's disease using resting-state fMRI and graph theory. *Clin Neurophysiol* 2015;126(11):2132–2141.
15. Palesi F, Castellazzi G, Casiraghi L, et al. Exploring patterns of alteration in Alzheimer's disease brain networks: a combined structural and functional connectomics analysis. *Front Neurosci* 2016;10:380.
16. Wang L, Xia M, Li K, et al. The effects of antidepressant treatment on resting-state functional brain networks in patients with major depressive disorder. *Hum Brain Mapp* 2015;36(2):768–778.
17. Hadley JA, Kraguljac NV, White DM, et al. Change in brain network topology as a function of treatment response in schizophrenia: a longitudinal resting-state fMRI study using graph theory. *NPJ Schizophr* 2016;2:16014.
18. Shin DJ, Jung WH, He Y, et al. The effects of pharmacological treatment on functional brain connectome in obsessive-compulsive disorder. *Biol Psychiatry* 2014;75(8):606–614.

19. Haneef Z, Levin HS, Chiang S. Brain graph topology changes associated with anti-epileptic drug use. *Brain Connect* 2015;5(5):284–291.
20. Folstein MF, Folstein SE, McHugh PR. "Mini-mental state". A practical method for grading the cognitive state of patients for the clinician. *J Psychiatr Res* 1975;12(3):189–198.
21. Mohs RC, Rosen WG, Davis KL. The Alzheimer's Disease Assessment Scale: an instrument for assessing treatment efficacy. *Psychopharmacol Bull* 1983;19(3):448–450.
22. Berg L. Clinical Dementia Rating (CDR). *Psychopharmacol Bull* 1988; 24(4):637–639.
23. Bucks RS, Ashworth DL, Wilcock GK, et al. Assessment of activities of daily living in dementia: development of the Bristol Activities of Daily Living Scale. *Age Ageing* 1996;25(2):113–120.
24. Cummings JL, Mega M, Gray K, et al. The Neuropsychiatric Inventory: comprehensive assessment of psychopathology in dementia. *Neurology* 1994;44(12):2308–2314.
25. Chao-Gan Y, Yu-Feng Z. DPARSF: a MATLAB toolbox for "pipeline" data analysis of resting-state fMRI. *Front Syst Neurosci* 2010;4:13.
26. Power JD, Barnes KA, Snyder AZ, et al. Spurious but systematic correlations in functional connectivity MRI networks arise from subject motion. *Neuroimage* 2012;59(3):2142–2154.
27. Ashburner J. A fast diffeomorphic image registration algorithm. *Neuroimage* 2007;38(1):95–113.
28. Tzourio-Mazoyer N, Landeau B, Papathanassiou D, et al. Automated anatomical labeling of activations in SPM using a macroscopic anatomical parcellation of the MNI MRI single-subject brain. *NeuroImage* 2002; 15(1):273–289.
29. Achard S, Bullmore E. Efficiency and cost of economical brain functional networks. *PLoS Comput Biol* 2007;3(2):e17.
30. He Y, Dagher A, Chen Z, et al. Impaired small-world efficiency in structural cortical networks in multiple sclerosis associated with white matter lesion load. *Brain* 2009;132(Pt 12):3366–3379.
31. Zhang J, Wang J, Wu Q, et al. Disrupted brain connectivity networks in drug-naive, first-episode major depressive disorder. *Biol Psychiatry* 2011; 70(4):334–342.
32. Suo X, Lei D, Li K, et al. Disrupted brain network topology in pediatric posttraumatic stress disorder: a resting-state fMRI study. *Hum Brain Mapp* 2015;36(9):3677–3686.
33. Lei D, Li K, Li L, et al. Disrupted functional brain connectome in patients with posttraumatic stress disorder. *Radiology* 2015;276(3):818–827.
34. Zhu J, Zhuo C, Liu F, et al. Distinct disruptions of resting-state functional brain networks in familial and sporadic schizophrenia. *Sci Rep* 2016; 6:23577.
35. Watts DJ, Strogatz SH. Collective dynamics of 'small-world' networks. *Nature* 1998;393(6684):440–442.
36. Rubinov M, Sporns O. Complex network measures of brain connectivity: uses and interpretations. *Neuroimage* 2010;52(3):1059–1069.
37. Rösler M, Anand R, Cicin-Sain A, et al. Efficacy and safety of rivastigmine in patients with Alzheimer's disease: international randomised controlled trial. *BMJ* 1999;318(7184):633–638.
38. Finkel SI. Effects of rivastigmine on behavioral and psychological symptoms of dementia in Alzheimer's disease. *Clin Ther* 2004; 26(7):980–990.
39. Matsuzono K, Sato K, Kono S, et al. Clinical benefits of rivastigmine in the real world dementia clinics of the Okayama Rivastigmine Study (ORS). *J Alzheimers Dis* 2015;48(3):757–763.
40. Zhao XH, Wang XB, Xi Q, et al. Small-worldness of functional networks in Alzheimer's disease. *Zhonghua Yi Xue Za Zhi* 2012;92(9):579–582.
41. Wolfson C, Oremus M, Shukla V, et al. Donepezil and rivastigmine in the treatment of Alzheimer's disease: a best-evidence synthesis of the published data on their efficacy and cost-effectiveness. *Clin Ther* 2002;24(6): 862–886; discussion 37.
42. Grahn JA, Parkinson JA, Owen AM. The role of the basal ganglia in learning and memory: neuropsychological studies. *Behav Brain Res* 2009; 199(1):53–60.
43. Middleton FA, Strick PL. Basal ganglia output and cognition: evidence from anatomical, behavioral, and clinical studies. *Brain Cogn* 2000; 42(2):183–200.
44. Alexander GE, DeLong MR, Strick PL. Parallel organization of functionally segregated circuits linking basal ganglia and cortex. *Annu Rev Neurosci* 1986;9:357–381.
45. Postuma RB, Dagher A. Basal ganglia functional connectivity based on a meta-analysis of 126 positron emission tomography and functional magnetic resonance imaging publications. *Cereb Cortex* 2006; 16(10):1508–1521.
46. Provost JS, Hanganu A, Monchi O. Neuroimaging studies of the striatum in cognition part I: healthy individuals. *Front Syst Neurosci* 2015;9:140.
47. Duffau H, Moritz-Gasser S, Mandonnet E. A re-examination of neural basis of language processing: proposal of a dynamic hodotopical model from data provided by brain stimulation mapping during picture naming. *Brain Lang* 2014;131:1–10.
48. Gil Robles S, Gatignol P, Capelle L, et al. The role of dominant striatum in language: a study using intraoperative electrical stimulations. *J Neurol Neurosurg Psychiatry* 2005;76(7):940–946.
49. Jiji S, Smitha KA, Gupta AK, et al. Segmentation and volumetric analysis of the caudate nucleus in Alzheimer's disease. *Eur J Radiol* 2013; 82(9):1525–1530.
50. Barber R, McKeith I, Ballard C, et al. Volumetric MRI study of the caudate nucleus in patients with dementia with Lewy bodies, Alzheimer's disease, and vascular dementia. *J Neurol Neurosurg Psychiatry* 2002; 72(3):406–407.
51. Rodríguez-Puertas R, Nilsson S, Pascual J, et al. 125I-galanin binding sites in Alzheimer's disease: increases in hippocampal subfields and a decrease in the caudate nucleus. *J Neurochem* 1997;68(3):1106–1113.
52. Oda Y, Nakanishi I. The distribution of cholinergic neurons in the human central nervous system. *Histol Histopathol* 2000;15(3):825–834.
53. Oh JD, Woolf NJ, Roghani A, et al. Cholinergic neurons in the rat central nervous system demonstrated by in situ hybridization of choline acetyltransferase mRNA. *Neuroscience* 1992;47(4):807–822.
54. Suzuki T, Kashima Y, Fujimoto K, et al. Regional differences in extracellular choline dependency of acetylcholine synthesis in the rat brain. *Neurosci Res* 1991;11(1):71–76.
55. Mesulam MM. Cholinergic circuitry of the human nucleus basalis and its fate in Alzheimer's disease. *J Comp Neurol* 2013; 521(18):4124–4144.
56. Winkler J, Suhr ST, Gage FH, et al. Essential role of neocortical acetylcholine in spatial memory. *Nature* 1995;375(6531):484–487.
57. Chavez C, Zaborszky L. Basal forebrain cholinergic-auditory cortical network: primary versus nonprimary auditory cortical areas. *Cereb Cortex* 2017;27(3):2335–2347.
58. Pearce BR, Palmer AM, Bowen DM, et al. Neurotransmitter dysfunction and atrophy of the caudate nucleus in Alzheimer's disease. *Neurochem Pathol* 1984;2(4):221–232.
59. Olson IR, McCoy D, Klobusicky E, et al. Social cognition and the anterior temporal lobes: a review and theoretical framework. *Soc Cogn Affect Neurosci* 2013;8(2):123–133.
60. Skipper LM, Ross LA, Olson IR. Sensory and semantic category subdivisions within the anterior temporal lobes. *Neuropsychologia* 2011; 49(12):3419–3429.
61. Hickok G, Poeppel D. The cortical organization of speech processing. *Nat Rev Neurosci* 2007;8(5):393–402.

62. Altmann U, Bohrn IC, Lubrich O, et al. The power of emotional valence—from cognitive to affective processes in reading. *Front Hum Neurosci* 2012;6:192.

63. Jimura K, Konishi S, Miyashita Y. Temporal pole activity during perception of sad faces, but not happy faces, correlates with neuroticism trait. *Neurosci Lett* 2009;453(1):45–48.

64. Royet JP, Zald D, Versace R, et al. Emotional responses to pleasant and unpleasant olfactory, visual, and auditory stimuli: a positron emission tomography study. *J Neurosci* 2000;20(20):7752–7759.

65. Parkinson C, Wheatley T. Relating anatomical and social connectivity: white matter microstructure predicts emotional empathy. *Cereb Cortex* 2014;24(3):614–625.

66. Damasio AR, Grabowski TJ, Bechara A, et al. Subcortical and cortical brain activity during the feeling of self-generated emotions. *Nat Neurosci* 2000;3(10):1049–1056.

67. Mathiak KA, Klasen M, Weber R, et al. Reward system and temporal pole contributions to affective evaluation during a first person shooter video game. *BMC Neurosci* 2011;12:66.

68. McClelland JL, Rogers TT. The parallel distributed processing approach to semantic cognition. *Nat Rev Neurosci* 2003;4(4):310–322.

69. Patterson K, Nestor PJ, Rogers TT. Where do you know what you know? The representation of semantic knowledge in the human brain. *Nat Rev Neurosci* 2007;8(12):976–987.

70. Chabardès S, Kahane P, Minotti L, et al. Anatomy of the temporal pole region. *Epileptic Disord* 2002;4(Suppl 1):S9–S15.

71. Pascual B, Masdeu JC, Hollenbeck M, et al. Large-scale brain networks of the human left temporal pole: a functional connectivity MRI study. *Cereb Cortex* 2015;25(3):680–702.

72. Tippett LJ, Miller LA, Farah MJ. Prosopamnesia: a selective impairment in face learning. *Cogn Neuropsychol* 2000;17(1):241–255.

73. Nakamura K, Kawashima R, Sugiura M, et al. Neural substrates for recognition of familiar voices: a PET study. *Neuropsychologia* 2001;39 (10):1047–1054.

74. Butler CR, Brambati SM, Miller BL, et al. The neural correlates of verbal and nonverbal semantic processing deficits in neurodegenerative disease. *Cogn Behav Neurol* 2009;22(2):73–80.

75. Lipczyńska-Łojkowska W, Ryglewicz D, Jedrzejczak T, et al. The effect of rivastigmine on cognitive functions and regional cerebral blood flow in Alzheimer's disease and vascular dementia: follow-up for 2 years. *Neurol Neurochir Pol* 2004;38(6):471–481.

76. Venneri A, Shanks MF, Staff RT, et al. Cerebral blood flow and cognitive responses to rivastigmine treatment in Alzheimer's disease. *Neuroreport* 2002;13(1):83–87.

77. Shapiro K, Hillstrom AP, Husain M. Control of visuotemporal attention by inferior parietal and superior temporal cortex. *Curr Biol* 2002;12(15): 1320–1325.

78. Nakamura K, Kawashima R, Sato N, et al. Functional delineation of the human occipito-temporal areas related to face and scene processing. A PET study. *Brain* 2000;123(Pt 9):1903–1912.

79. Wezenberg E, Verkes RJ, Sabbe BG, et al. Modulation of memory and visuospatial processes by biperiden and rivastigmine in elderly healthy subjects. *Psychopharmacology (Berl)* 2005;181(3):582–594.

80. Mossello E, Tonon E, Caleri V, et al. Effectiveness and safety of cholinesterase inhibitors in elderly subjects with Alzheimer's disease: a "real world" study. *Arch Gerontol Geriatr Suppl* 2004;297–307.

81. Fornito A, Zalesky A, Bullmore ET. Network scaling effects in graph analytic studies of human resting-state FMRI data. *Front Syst Neurosci* 2010;4:22.

82. Zalesky A, Fornito A, Harding IH, et al. Whole-brain anatomical networks: does the choice of nodes matter? *Neuroimage* 2010;50(3):970–983.

83. Serra L, Mancini M, Cercignani M, et al. Network-based substrate of cognitive reserve in Alzheimer's disease. *J Alzheimers Dis* 2017;55(1):421–430.